



Structural and physical properties of the high pressure perovskite layered $\text{Sr}_4\text{Cr}_3\text{O}_{10}$ chromate

Justin Jeanneau^{a,b,*}, Christophe Lepoittevin^{a,b}, André Sulpice^{a,b}, Stéphanie Kodjikian^{a,b}, Pierre Toulemonde^{a,b}, Manuel Núñez-Regueiro^{a,b}

^a Université Grenoble-Alpes, Institut Néel, F-38000 Grenoble, France

^b CNRS, Institut Néel, F-38000 Grenoble, France

ARTICLE INFO

Keywords:

High pressure – high temperature synthesis
Layered materials
Precession Electron Diffraction
Powder X-ray diffraction
Magnetization
Electrical transport

ABSTRACT

We report on the structure and physical properties of a bidimensional chromate, $\text{Sr}_4\text{Cr}_3\text{O}_{10}$, the $n=3$ member of the Ruddlesden-Popper $\text{Sr}_{n+1}\text{Cr}_n\text{O}_{3n+1}$ series. For the first time, using complementary x-ray powder diffraction and electron diffraction data, we have solved its layered crystallographic structure. Our study shows also that this high pressure phase is insulating and antiferromagnetic below $T_N=280$ K, a similar behavior already observed for $n=1, 2$ and $n=+\infty$ members.

1. Introduction

The layered oxides derived from the perovskite structure constitute a large family of compounds that yields an extremely rich physics. In such a structure the MO_2 (with M = transition metal element) layer always plays an essential role. For the case of 3d elements this family was at the origin of the discovery of high T_c superconductivity in the cuprates [1] or giant magnetoresistance in manganates [2,3]. Recently we have started a more detailed study of the different members of the Ruddlesden-Popper series based on chromium, $\text{Sr}_{n+1}\text{Cr}_n\text{O}_{3n+1}$ [4]. Few reports exist in the literature on these chromates because High Pressure – High Temperature (HP-HT) is needed for their synthesis. In $\text{Sr}_3\text{Cr}_2\text{O}_7$ ($n=2$) we have reported an anomalous asymmetric distortion of the CrO_6 octahedra associated to simultaneous orderings of the orbital and spin degrees of freedom [5]. We focus here on the isolation of the phase $\text{Sr}_4\text{Cr}_3\text{O}_{10}$ ($n=3$) and its structural and magnetic characterizations. It was previously only detected as an intergrowth in high resolution transmission electron microscopy (HRTEM) images of $\text{Sr}_3\text{Cr}_2\text{O}_7$ [6]. Thanks to a combined X-ray and electron diffraction study, we have resolved the crystallographic structure of this $n=3$ member. In addition, we show that $\text{Sr}_4\text{Cr}_3\text{O}_{10}$ (Sr4310) is an insulator with an antiferromagnetic (AFM) transition at $T_N=280$ K.

2. Experimental

The synthesis of layered chromates is difficult, as it requires HP-HT

techniques. Our samples were prepared using a large volume press with toroidal “Conac 28” anvils [7,8]. A stoichiometric mixture (4:3) of SrO (Sigma Aldrich 99%) and CrO_2 (Sigma Aldrich 99%) was pressed into a pellet and introduced in a gold capsule. Our polycrystalline samples were treated at HP-HT in the 4–6 GPa range and 1100 °C for 30 min. The conditions were optimized to increase the amount of the Sr4310 phase.

Powder X-ray diffraction experiments were performed on a D5000T diffractometer working with the Cu K_α wavelength ($\lambda_\alpha = 1.5406$ Å). Data were collected at room temperature, in a 2θ angular range from 10.00° to 90.32° , with a 0.032° step size.

For TEM analysis, the specimen was prepared by crushing a small piece of sample in an agate mortar containing ethanol, and a drop of the suspension was deposited on a copper grid covered with a holey carbon film. Electron transmission microscopy was performed on a LaB₆ Philips CM300ST Transmission Electron Microscope (TEM) operating at 300 kV, equipped with a $\pm 30^\circ$ double tilt sample holder and the Nanomegas spinningstar precession device (with a precession angle of 2.5° for our experiments). Images and Selected Area Electron Diffraction with and without Precession (SAED and PED) patterns were recorded using a F416 TVIPS camera, and the Energy Dispersive Spectroscopy (EDS) spectra were recorded on a Bruker Silicon Drift Detector. Reflection intensities extraction on PED patterns was performed using ELD module from CRISP software and merging process was carried out with TRIPLE, both software belong to the Calidris package [9]. The final hkl dataset was used as an input in the direct

* Corresponding author at: Université Grenoble-Alpes, Institut Néel, F-38000 Grenoble, France.
E-mail address: justin.jeanneau@neel.cnrs.fr (J. Jeanneau).

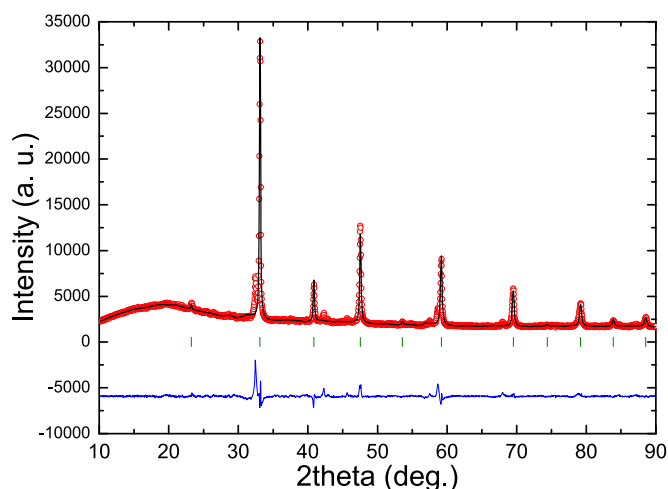


Fig. 1. Rietveld refinement of the powder XRD pattern taking into account only the SrCrO_3 phase. The pattern exhibits the experimental (red circles), calculated (black line) and difference (blue line) curves in the range $2\theta = 10.2^\circ - 90.3^\circ$ ($R_{\text{Bragg}} = 5.17\%$ and global $\chi^2 = 19.2\%$). Green vertical markers refer to the calculated positions of the Bragg reflections for SrCrO_3 . (For interpretation of the references to color in this figure legend, the reader is referred to the web version of this article.)

method structure determination software SIR2011 [10] to calculate “ab initio” the structural model.

The magnetic properties of our samples were measured in a Metronique Ingenierie SQUID with a sensitivity of 10^{-7} emu at low field and 10^{-5} emu at high field. Electrical resistivity measurements were performed using the four contacts (with epoxy-silver paint) technique using a DC current of 10 μA .

3. Results and discussion

We now focus our discussion on the properties of our sample containing the maximal amount of $\text{Sr}_4\text{Cr}_3\text{O}_{10}$, around $\sim 23\%$ (see results of the final Rietveld refinement below), for the P,T conditions used (i.e. elaborated at 4 GPa and 1100 $^\circ\text{C}$). Its powder XRD pattern and the corresponding Rietveld refinement are shown on Fig. 1. Most of the main diffraction peaks can be indexed with the perovskite structure SrCrO_3 . Nevertheless, the reliability factors of the refinement are not good ($R_{\text{Bragg}} = 5.17\%$ and global $\chi^2 = 19.2\%$). Indeed, the remaining Bragg peaks, evidenced on the difference curve (between the calculated

and observed intensities), do not fit to the precursors nor any other phase present in the crystallographic database. They correspond to the reflections of the $\text{Sr}_4\text{Cr}_3\text{O}_{10}$ phase not overlapped with the ones of the perovskite. By analogy with the isostructural $\text{Sr}_4\text{Ti}_3\text{O}_{10}$ ($a = 3.90 \text{ \AA}$ and $c = 28.1 \text{ \AA}$) of the Ti-based series $\text{Sr}_{n+1}\text{Ti}_n\text{O}_{3n+1}$ [11,12] a first estimation of the tetragonal lattice parameters of $\text{Sr}_4\text{Cr}_3\text{O}_{10}$ can be made: $a = 3.82(2) \text{ \AA}$ and $c = 27.8(5) \text{ \AA}$.

3.1. Imaging, EDS analysis and SAED

TEM imaging and EDS analysis were carried out on over 40 particles, exhibiting three types of particles, easily recognizable thanks to their shape and their cationic ratio. In Fig. 2(a) the rods surrounded by red hatched circles correspond to crystallized particles with the cationic ratio: $\text{Sr}/\text{Cr} \approx 57\%/43\%$ (the $\text{Sr}_4\text{Cr}_3\text{O}_{10}$ phase), the bigger crystallized particles correspond to the cationic ratio $\text{Sr}/\text{Cr} \approx 50\%/50\%$ (majority perovskite SrCrO_3 phase) and the “stringy-shaped” particles (100% Sr from EDS and amorphous phase according to SAED carried out on it) are very likely hydrated SrO precursor $\text{Sr}(\text{OH})_2(\text{H}_2\text{O})_x$.

Several ED patterns of the $\text{Sr}_4\text{Cr}_3\text{O}_{10}$ were recorded in zone axis by tilting around crystallographic axes for the unit cell and extinction conditions determination. The reconstruction of the reciprocal space confirmed the tetragonal unit cell with the parameters $a \approx 3.9 \text{ \AA}$ and $c \approx 28 \text{ \AA}$ (Fig. 2(b)) previously determined by XRD. The extinction conditions on hkl reflections are consistent with a body-centered I lattice type and no other extra conditions were observed..

3.2. Precession electron diffraction

Extraction of reflection intensities of each PED pattern was performed by integrating the intensity of each reflection after subtracting the background noise. Consequently 5 different datasets were created from the zone axes PED patterns $[010]$, $[1-40]$, $[1-30]$, $[1-20]$, $[2-30]$ (Fig. 3) and merged using the common reflections between patterns. This process gave rise to reliability factor R_{merge} lower than 8%, confirming the good homogeneity between intensities of the common reflections. A second merge step was carried out by applying the most symmetrical space group $I4/mmm$, giving rise to 556 independent reflections with a satisfactory R_{sym} of 2.7%.

Combining the EDS cationic ratio $\text{Sr}/\text{Cr} = 57\%/43\%$ with the attribution of 2+ valency for strontium and 4+ for chromium, the chemical formula $\text{Sr}_{1.14}\text{Cr}_{0.86}\text{O}_{2.86}$ was deduced. To calculate the number of atoms per unit cell, the number of atoms in the cubic

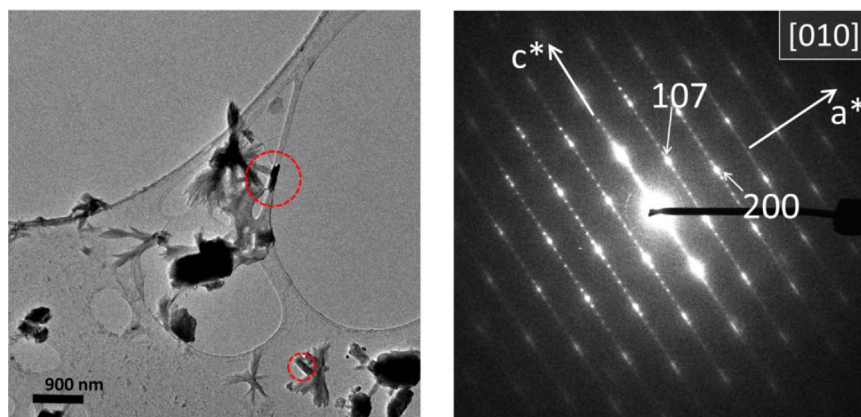


Fig. 2. (a) Low resolution TEM image of the particles contained in the powder. The small needle-shaped particles highlighted by red dashed circles correspond to the $\text{Sr}_4\text{Cr}_3\text{O}_{10}$ phase. (b) $[010]$ Zone axis SAED pattern of a $\text{Sr}_4\text{Cr}_3\text{O}_{10}$ particle. (For interpretation of the references to color in this figure legend, the reader is referred to the web version of this article.)

Download English Version:

<https://daneshyari.com/en/article/5153685>

Download Persian Version:

<https://daneshyari.com/article/5153685>

[Daneshyari.com](https://daneshyari.com)